

Screening of Novel Li-Air Battery Catalyst Materials by a Thin Film Combinatorial Materials Approach

*John G. Hauck and Paul J. McGinn**

Supporting information

X-Ray Diffraction

XRD characterization of the Pt-Mn-Co system showed that compositions exhibited the phases expected from the corresponding phase diagrams. Diffraction patterns from the Pt-Co binary system within the library are illustrative in this regard (Figure S5a). For Pt compositions of 0-43 at%, the Co-Pt binary films were of the Co-phase with Pt in solid solution. The Co-phase crystal lattice expanded with increasing Pt composition, which caused the Co (111) peak to shift to lower values of 2θ in accordance with Vegard's law. Similarly, films with compositions of 57-100 at% Pt were Pt solid solutions, with the Pt (111) peak shifting as the Pt composition increased. Films with Pt content between 43-57 at% were composed of the Co-Pt alloy phase as evidenced by the new diffraction peak at 41.52° . This peak also shifted to higher diffraction angles as the Pt composition increased from 43 at% to 57 at% in accordance with Vegard's law. The diffraction pattern for $\text{Pt}_{12}\text{Mn}_{44}\text{Co}_{44}$ (Figure S5b) shows only a peak corresponding to the MnCo phase (in addition to the TiN underlayer). The MnCo (222) peak at $2\theta = 94.281^\circ$ is shifted

from the expected value of 95.3176° ,¹ corresponding to an expansion of the crystal lattice which presumably is due to the incorporation of Pt. Due to the effects of film texture and thickness other peaks from this phase could not be observed.

FIGURES

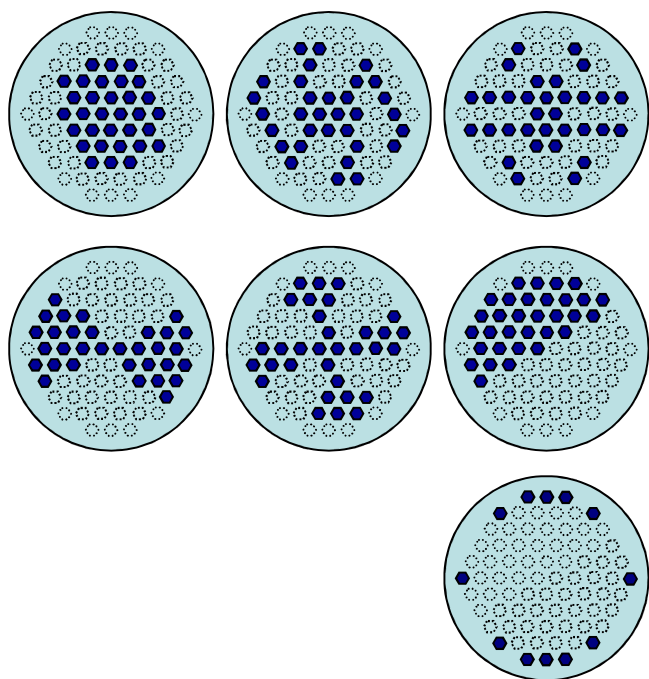


Figure S1. Shadow masks used in sputtering system to generate combinatorial libraries.

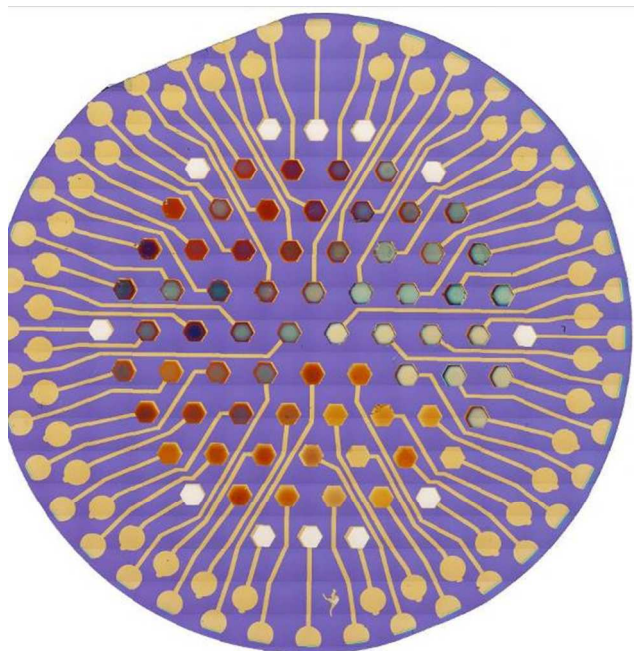


Figure S2. Micrograph of fully fabricated library wafer before electrochemical testing.

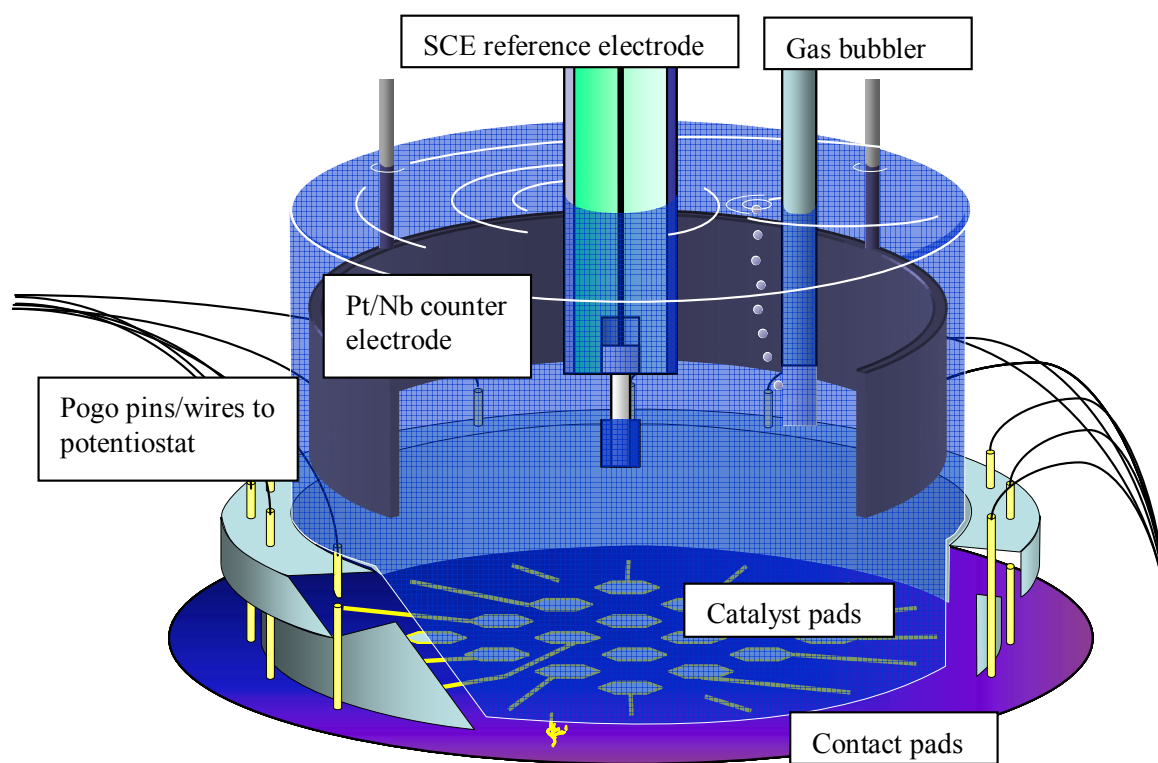


Figure S3. Diagram of electrochemical cell used for high-throughput screening.

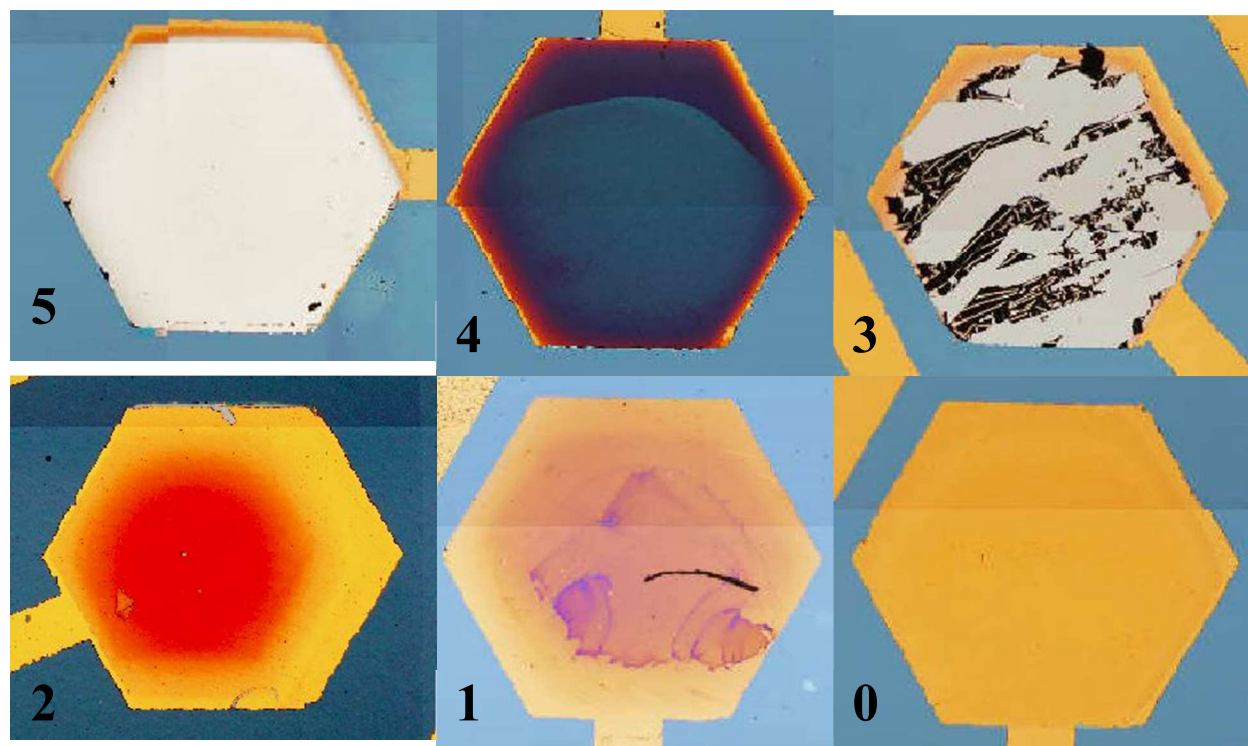
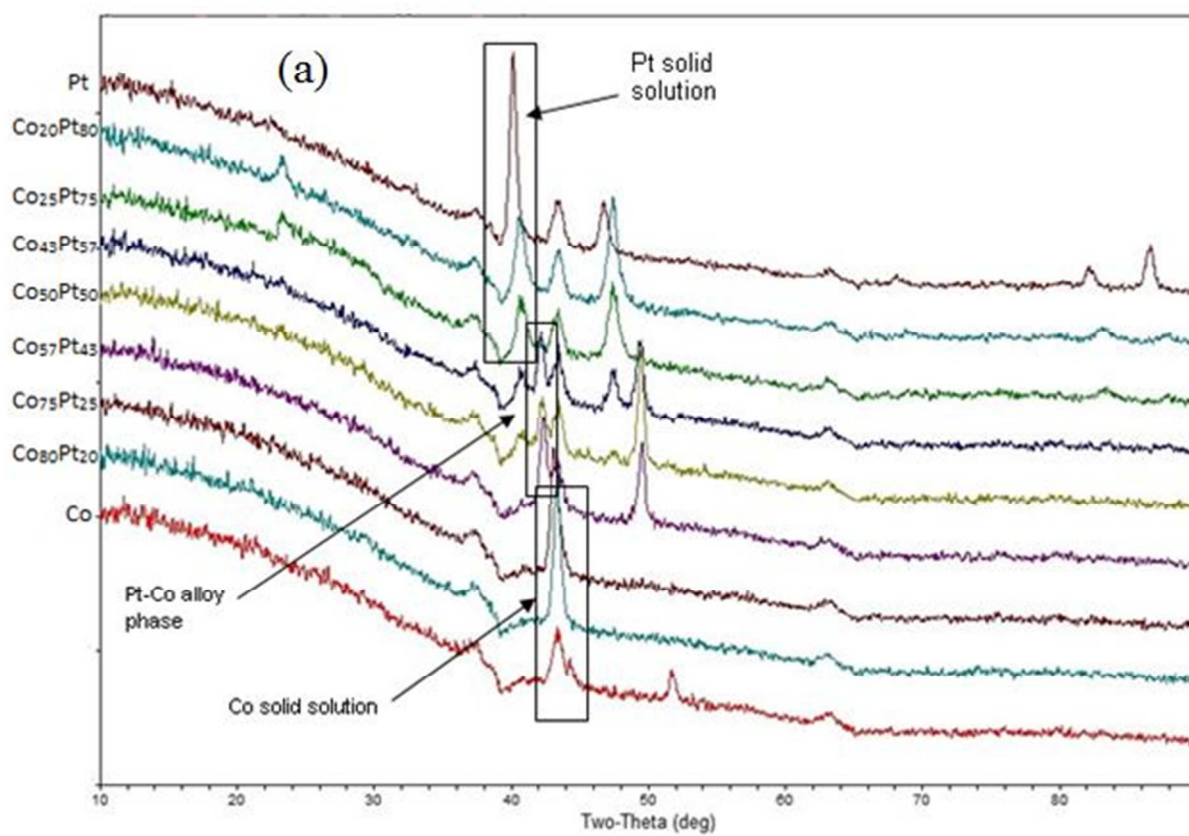


Figure S4. Examples of corrosion score rankings. Numbers correspond to corrosion scores identified in Table S1.



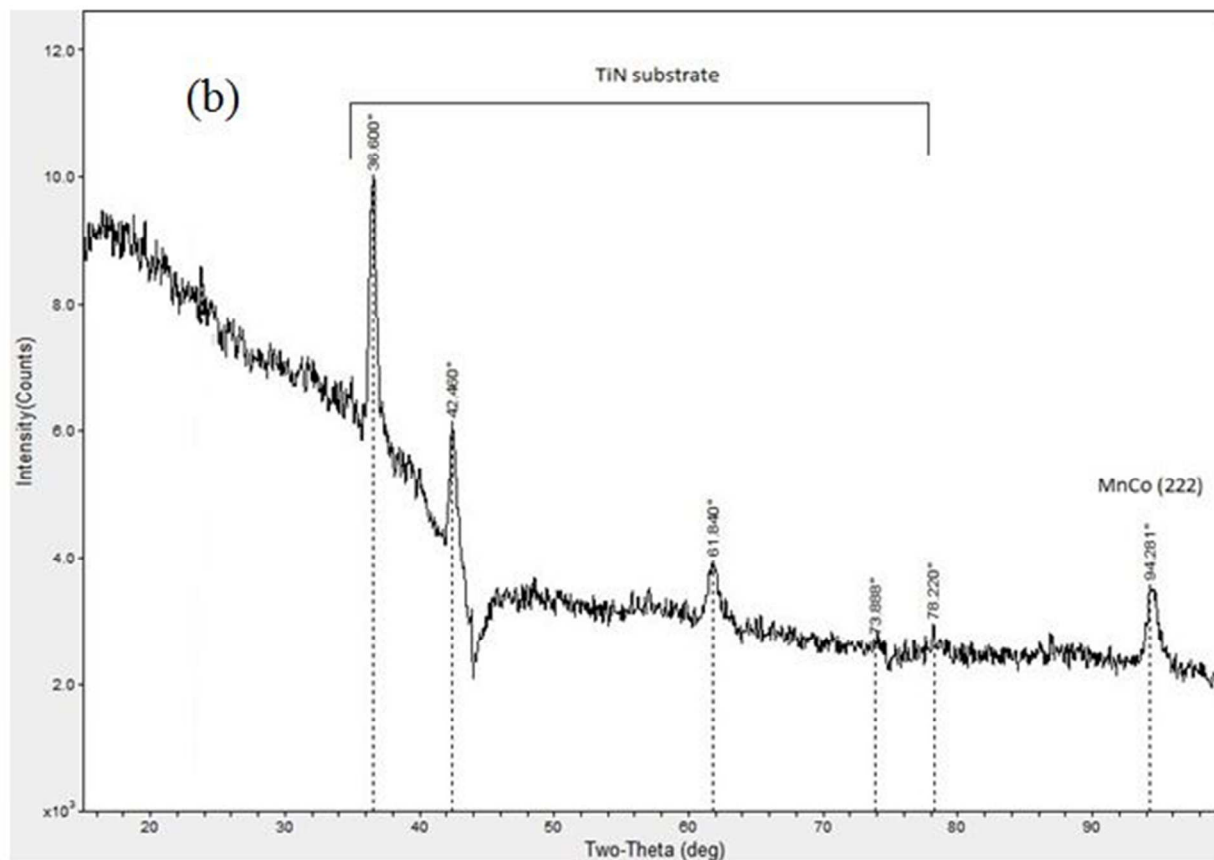


Figure S5. (a) X-ray diffraction patterns of Pt-Co alloys from the Pt-Mn-Co system. (b) Diffraction pattern for $\text{Pt}_{12}\text{Mn}_{44}\text{Co}_{44}$.

TABLES

Table S1. Corrosion resistance scores.

Score	Criterion
5	No difference before and after testing
4	Some discoloration
3	Spalled, ragged patches have flaked off
2	Perimeter is shrinking
1	Spalled and shrinking
0	Vanished, no trace of the catalyst remains

REFERENCE

- (1) Cable, J. W.; Tsunoda, Y. *J. Magn. Magn. Mater.* **1995**, *140–144, Part 1*, 93–94.